Effects of microgeometry and surface relaxation on NMR pulsed-field-gradient experiments: Simple pore geometries

Partha P. Mitra* and Pabitra N. Sen
Schlumberger-Doll Research, Old Quarry Road, Ridgefield, Connecticut 06877-4108
(Received 24 May 1991; revised manuscript received 14 August 1991)

We derive an expression for the magnetization $M(k,\Delta)$ in a pulsed-field-gradient experiment for spins diffusing in a confined space with relaxation at the pore walls. Here $\mathbf{k} = \gamma\delta\mathbf{g}$, δ = pulse width, $\mathbf{g}$ = gradient strength, γ = the gyromagnetic ratio, and Δ is the time between gradient pulses. We show that the deviation of $-\ln[M(k,\Delta)/M(0,\Delta)]$ from quadratic behavior in k in experiments in porous media can be a more sensitive probe of the microgeometry (size, connectivity, size distribution, shape, etc.), than either the enhancement of $1/T_1$ over the bulk water value, or the macroscopic diffusion coefficient, which is derived from the slope of $-\ln[M(k,\Delta)/M(0,\Delta)]$ at small k^2, in the limit of large Δ. We propose some simple models of randomly oriented tubes and sheets to interpret the k dependence of the amplitude beyond the leading small-k quadratic behavior. When the macroscopic diffusion coefficient is unobtainable, due to the decay, the present considerations should be useful in extracting geometrical information. The effective diffusion constant derived from NMR exactly equals that derived from electrical conductivity only when the surface relaxivity is zero, but can be close to each other in favorable circumstances even for finite surface relaxivity. Exact solutions with partially absorbing boundary conditions are obtained for a slab and a sphere to infer that the normalized amplitude $M(k,\Delta,\rho)/M(0,\Delta,\rho)$ depends only *weakly* on the surface relaxivity ρ for monodisperse convex-shaped pores in the parameter ranges of interest. We also obtain expressions for the mean lifetime of the amplitude in the geometries considered.

I. INTRODUCTION

Spin echo measurements are routinely used for studying molecular diffusion in fluids.[1,2] When the diffusion is confined by the presence of obstacles, the experiments yield information about the confining geometry[2-10] as seen by the diffusing particle. In porous media, precisely such information, i.e., length scales, such as pore and throat sizes, and geometric factors, such as tortuosity and connectivity, determine the transport and other properties. There has been a lot of interest recently in using NMR techniques to obtain information on microgeometry, the interest being in part due to the noninvasive nature of these measurements.

The main purpose of this paper is to show that in a pulsed-field-gradient (PFG) experiment, the full k ("momentum") dependence contains much more information about the microgeometry than just the usual diffusion coefficient, which is derived from the k^2 dependence of the logarithm of the normalized echo amplitude at small k. We give examples to show the influences of size, the local anisotropy of the pore space, and of a distribution of sizes on the k^4 term. The true macroscopic diffusion coefficient (i.e., the diffusion constant measured in the limit of large Δ for a connected pore space) contains the valuable information of tortuosity, but not the pore size. Furthermore, the method suggested here can give geometry information when the enhanced decay forbids a successful extraction of the macroscopic diffusion coefficient. The importance of the pulsed-gradient experiment from a theoretical point of view is that it directly measures the Fourier transform of the diffusion propagator in pore space.

In order to interpret data it is a prerequisite to account for the decay at pore walls which dominates the relaxation in many porous media. We give here the proper formulation which takes into account the surface relaxation. The presence of surface relaxers enters as a partially absorbing boundary condition for the magnetization at the pore wall. Considering the importance of surface relaxivity, it is surprising that the partially absorbing boundary condition has previously not been treated properly for field gradient experiments, even in the context of the effective diffusion coefficient.

In addition to the investigation of the effective diffusion coefficient using field gradients, there has been much effort in obtaining geometrical information using the enhancement[11-18] in the NMR longitudinal decay rate $1/T_1$. The increase in decay rate in rocks generally comes from the paramagnetic impurities on the pore walls. The longitudinal decay rate is enhanced by relaxers on pore walls in proportion to the surface to volume ratio,[16,18] i.e.,

$$\frac{1}{T_1} \approx \frac{\delta_x S}{T_{1S} V} = \frac{\rho S}{V}, \tag{1.1}$$

where T_{1S} is the enhanced relaxation within a distance δ_x, ρ is a surface relaxivity, S is surface area, and V the pore volume. The principal difficulty in relating pore size to the relaxation rate is the appearance of an unknown

parameter ρ.

Apart from an unknown ρ, T_1 is not a sensitive probe of the geometry of the pore space—it has no information about tortuosity or connectivity. The T_1 data cannot even distinguish between connected and disconnected pores. In fact, it is customary[14] to analyze the relaxation data in terms of a collection of isolated pores and use the size data to infer the rock permeability from an empirical statistical correlation. The permeability of a system of isolated pores is zero. The permeability is a key parameter in the oil industry and any estimation of it is valued. Isolated pores have discrete spectrum and localized eigenmodes. Even though a continuum of isolated pore sizes can mimic the continuous spectrum of a connected system, the modes are still localized. The PFG amplitude is sensitive to the eigenfunctions in addition to the spectrum, and in principle, is a valuable probe of the geometric information. While the macroscopic diffusion coefficient seems attractive, it may be unobtainable due to the decay of the signal.

Since the spin echo measurements are directly influenced by the confining geometry, as seen by the walker, it is natural to use these measurements for obtaining information relating to transport. In particular, pulsed gradient measurements have been used or proposed to obtain similar information.[2–11,19–28] However, the previous studies have been confined chiefly to the effective diffusion constant, which is derived from the small-k dependence of the amplitude, $M(k,\Delta)$. Here $\mathbf{k} = \gamma\delta\mathbf{g}$, δ = pulse width, $\mathbf{g}$ = gradient strength, γ = the gyromagnetic ratio, Δ is the interpulse separation. For the PFG experiment this means that a diffusion coefficient is extracted from the k^2-dependent term:

$$\ln\left(\frac{M(k,\Delta)}{M(0,\Delta)}\right) = -k^2\bar{D}(\Delta)\Delta. \tag{1.2}$$

Clearly, the "diffusion coefficient" $\bar{D}(\Delta)$ will be zero for an isolated pore in the long time limit: thus it carries the information on the connectedness of pores. The quotes have been used to indicate that the diffusion coefficient cannot be defined unless the displacement squared grows linearly with time, which is certainly not the case for an isolated pore. For a connected pore space D_{eff} (the long time effective diffusion constant) has the valuable information of the tortuosity. Among others, Vinegar and Rothwell[8] have proposed that, as the interpulse time Δ increases, the effective diffusion coefficient will change from its molecular value to the macroscopic value—the latter being related to the former by porosity and formation factor F,

$$D_{\text{eff}} = \frac{D}{F\phi}, \quad F = \frac{\sigma_w}{\sigma}. \tag{1.3}$$

Here ϕ is the porosity and F the formation factor, which is the conductivity of the saturating fluid σ_w divided by the conductivity σ of the fluid-saturated porous medium, which is made up of insulating grains. We have corrected for the factor of ϕ which is missing in the original reference.[8] Equation (1.3) follows from the Einstein relationship between the diffusion coefficient and the conductivity when applied to porous media.[29] Thus, the PFG experiment gives a possible way of estimating F. As noted by Vinegar and Rothwell,[8] the formation factor F is perhaps the most valuable geometrical factor which is used in the oil industry to estimate hydrocarbon fraction. However, there are two points which we need to bear in mind. First, the parameters involved for a typical rock show that the signal is likely to decay before the spin has diffused across a sufficient number of pores needed to see the macroscopic diffusion constant. For example, in a sandstone with a typical pore size of 5 μm, the time required to traverse, say four pores, is about 0.2 s, using $D = 2\times10^{-5}$ cm s^{-2} for water at room temperature. The typical value of T_1 is of the same order, and T_2 even shorter. The main problem is that the decay time is controlled by the small pores and while there may be sufficient time to traverse several small pores (due to small $\rho a/D$), macroscopic diffusion requires traversing several small and large pores.

In order to overcome this difficulty of lifetime, we suggest that one should study the deviation of the k dependence of the amplitude from its (small) k^2 behavior. This deviation is an important characterization of the microgeometry of the porous medium, especially since this deviation happens even if the observation time is not long enough to see the asymptotic diffusion constant. We analyze this deviation by the means of some simple models. Even the simple models reveal that deviation from k^2 dependence contains much more detailed information than the T_1 enhancement.

The second point is that the electrical formation factor in Eq. (1.3), in the absence of any surface conduction, will be related to that derived from NMR if $\rho \equiv 0$. Only then are the governing equations *and* the boundary conditions for the underlying diffusion problems identical for the NMR and the electrical cases. It is obvious that if the pores were connected by long thin necks with high values of ρ, the decay in the necks will effectively isolate the pores. Thus the role of surface relaxivity needs to be properly incorporated in the analysis. The study of connected geometries with surface relaxivity will be reported elsewhere.

In this paper we consider the combined effect of confining geometries and nonzero ρ on the pulsed gradient measurements in simple geometries. Some limiting results have been obtained in the literature for this problem, e.g., Frey *et al.*[3] obtain the solution for a slab for perfectly absorbing boundary conditions $\rho = \infty$. Lipsicas, Banavar, and Willemesen[6] make an approximation by taking the decay in a single pore to be a product of two terms. The first term is the decay amplitude calculated at zero (pulsed) field gradient but with a finite surface relaxivity ρ, and the second term is the amplitude calculated in the presence of a finite (pulsed) field gradient but with $\rho = 0$. While our calculations show that their approximation is valid [see Eqs. (6.12) and (6.13) below] for their model system, an analysis of the parameter values show that their result is probably inapplicable to many systems of interest (e.g., carbonate and sandstone rocks in an appropriate gradient range).

The effects of restricted diffusion were first consid-

ered by Wayne and Cotts[19] and by Robertson[20] for the Hahn[1] echo experiment (with a constant gradient) in a slab geometry with reflecting boundary conditions. Wayne and Cotts[19] also analyzed Woessner's[4] data on rocks using the result for slabs. The pulsed-field-gradient method[21–23] was first applied to the case of restricted diffusion by Tanner and Stejskal.[21–23] Numerous similar studies exist in the literature in related systems (see Ref. 2 for a review). To remove the effects of internal field gradients due to susceptibility inhomogeneities, which causes T_2-like decay to be much faster than T_1-like decay, the method of stimulated echos[22,24,2] is useful. Some studies exist on the k^2 dependence of the amplitude arising out of geometric effects, either due to anisotropic diffusion[21,27] or due to a distribution of pore sizes.[28]

The results obtained in this paper are the following. We first describe the general formulation of the decay amplitude in a pulsed-field-gradient-stimulated echo experiment in Sec. II. We also set out the cumulant expansion which we use to go beyond the traditional k^2 dependence. In Sec. III we study the k^2 dependence of the decay amplitude for fluid in confined and connected geometries. In Sec. IV we show the influence of size distribution and shape on the k^4 term in the case of isolated pores. We present in Sec. V models of randomly oriented sheets or tubes to model the k dependence of the decay amplitude for fluid in a rock matrix. These models capture some of the essential physics involved in the deviation of $\ln[M(k,\Delta,\rho)/M(0,\Delta,\rho)]$ from quadratic behavior in k, even for small k, which is seen in experiments. The exact results for planar and spherical pores are given in Sec. VI. The exact solutions and the cumulant expansions show that for an isolated convex-shaped pore, the decay amplitude depends only weakly on the surface relaxivity ρ apart from an overall normalization at zero gradients, i.e., $M(k,\Delta,\rho)/M(0,\Delta,\rho)$ is relatively independent of ρ. In Sec. VII we discuss the effects of random local fields, which arise due to the difference in magnetic susceptibilities of water and the porous medium. Section VIII is the concluding section.

We note that the problem treated in this paper is formally identical to the problem of particles leaving a pore space by passing through permeable walls, with the identification $\rho = \kappa$ where κ is the permeability through the wall.[2] It is assumed that the particles that have left the pore space no longer contribute to the signal.

II. GENERAL FORMULATION

In this section we derive the expression for magnetization with an appropriate boundary condition and set up the systematic procedure of obtaining geometrical information via the cumulant expansion.

The pulse sequence for which our results are derived is shown in Fig. 1 (see Refs. 2 and 22 for more details). We shall make the simplifying assumption $\delta, \tau_1 \to 0$, $g \to \infty$ keeping the product δg constant. In this limit we make two major simplifications: firstly, we can neglect the diffusion of the particles during the time when the magnetization is in the x-y plane and secondly in this limit

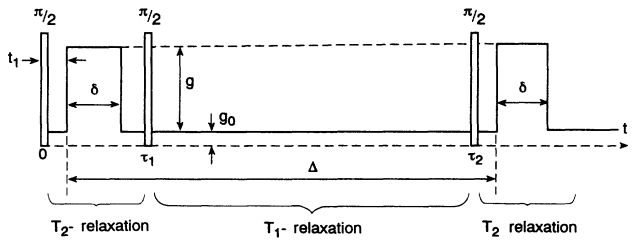

FIG. 1. The Tanner pulse sequences of a stimulated pulse echo (Refs. 2 and 22): g_0 is a constant background field gradient and g is the applied field gradient $\delta g >> \tau_1 g_0$.

we can neglect the effects of any spatial randomness in the local Larmor frequency in the porous material. This simplification makes it possible to consider the influence of microgeometry separately from other complications. Throughout this paper we will consider stimulated pulse echo (Fig. 1) and the surface relaxivity which corresponds to T_1. There are many systems, such as some carbonate rocks, where the susceptibility difference is small, and the internal field inhomogeneities are negligible. In those cases, the simple PFG echo[21,2] can be used (for which the appropriate surface decay rate corresponds to that for T_2). If the inhomogeneities are too large, they may even prevent the use of these techniques. We will return to the effects of random internal inhomogeneities in the magnetic field in Sec. VII.

A. The magnetization with partially absorbing boundary condition

The importance of the pulsed gradient experiment from a theoretical point of view is that it directly measures the Fourier transform of the diffusion propagator of a walker in the pore space with an average over the initial position of the walker implied. The presence of surface relaxers enters as a partially absorbing boundary condition for the walkers. In the limit $\delta, \tau_1 \to 0$, $|\mathbf{g}| \to \infty$ with $\delta\mathbf{g}$ fixed, the expression for the decay amplitude, with the bulk decay $\exp(-\Delta/T_{1B})$ factored out, is given by

$$M(\mathbf{k},\Delta) = \frac{1}{V}\int d\mathbf{r}\, d\mathbf{r}' G(\mathbf{r},\mathbf{r}',\Delta) e^{-i\mathbf{k}\cdot(\mathbf{r}-\mathbf{r}')},$$

$$\mathbf{k} = \gamma\delta\mathbf{g}, \quad (2.1)$$

where G satisfies the diffusion equation in the interior of the pore space with diffusion constant D

$$\frac{\partial G(\mathbf{r},\mathbf{r}',t)}{\partial t} = D\nabla^2 G(\mathbf{r},\mathbf{r}',t), \quad t > 0,$$
$$G(\mathbf{r},\mathbf{r}', t = 0^+) = \delta(\mathbf{r}-\mathbf{r}'), \quad (2.2)$$

and the boundary conditions at the surface Σ with an outward normal $\hat{\mathbf{n}}$ are

$$D\hat{\mathbf{n}}\cdot\nabla G(\mathbf{r},\mathbf{r}',t) + \rho G(\mathbf{r},\mathbf{r}',t)\,|_{\mathbf{r}\epsilon\Sigma} = 0. \quad (2.3)$$

The amplitude can be written more concisely using the language of random walks, since $G(\mathbf{r},\mathbf{r}',t)$ is the conditional probability of finding a random walker at $\mathbf{r},t$, which was released at $\mathbf{r}', t=0$:

$$M(k,\Delta) = \langle e^{-i\mathbf{k}\cdot[\mathbf{r}(0)-\mathbf{r}(\Delta)]}\rangle_{un}, \tag{2.4}$$

where $\langle\cdots\rangle_{un}$ denotes an average over random walks originating from $\mathbf{r}(0)$ and terminating at $\mathbf{r}(\Delta)$ in time Δ, the initial and final positions being integrated over. We have used a subscript *un* to distinguish it from the angular brackets which are used below to denote averages normalized to their values at $\mathbf{k}=0$. The random walkers contributing to the average diffuse freely in the interior of the pore space and are either reflected or absorbed at the pore walls with fixed probabilities given in terms of ρ.

It is important to note when the approximations made in deriving the above expressions fail. The approximation that the gradient pulses are infinitely sharp is not valid if the diffusion length $\sqrt{D\delta} > 1/(\gamma g\delta)$. In addition if the length $\sqrt{D\delta}$ is larger than the typical pore size, then the particles hit the wall during the pulse. Thus, for a 5-ms pulse, using $D = 2\times10^{-5}\text{cm}^2/\text{s}$, corrections are needed for the finite pulse size when the pore sizes are smaller than 3 μm. The effect of a finite pulse width is not difficult to treat if the diffusion is free, and the problem can be solved exactly.[22] However, when the diffusion is restricted, the problem becomes much harder, except in the second-cumulant approximation.[19,20,25,26] Therefore, the correction for a finite pulse width cannot be made using the corresponding correction for free diffusion. The other approximation that has been made is that the magnetization is initially spatially homogeneous. This will break down if there is significant phase evolution before the application of the first gradient pulse due to internal-field-gradient inhomogeneities, or surface relaxation. We will assume that this is not the case.

B. Dimensional considerations

Simple dimensional considerations give much insight. We propose that the "momentum" ($\gamma\delta g$) dependence of amplitude at fixed time reveals features of the characteristic length associated with a gradient pulse $1/(\gamma\delta g)$, provided that the diffusion length $\sqrt{D\Delta}$ is larger than this characteristic scale. Of course, Δ is limited by the decay time of the magnetization.

Let us first assume that there is a single length scale a in the confining geometry (e.g., sphere radius, tube diameter, or slab thickness). To be specific, we will keep in mind a sandstone rock, and consider PFG experiments on water protons in the pore spaces. For a typical pore size in a sandstone we may take $a \sim 2$–5 μm. For experiments at a fixed time (pulse separation) Δ, another relevant length is the diffusion length $l_D = \sqrt{D\Delta} \sim 4$–$32$ μm, for $\Delta \sim 10$–500 ms, $D = 2\times10^{-5}$ cm^2 s^{-1} for water at room temperature. There are two time scales: the diffusion time $\tau_D = a^2/D \sim 0.002$–$0.0125$ s, and the surface relaxation time $\tau_\rho = a/\rho \sim 0.2$–$0.5$ s with $\rho = 10^{-3}$ cm/s, a value which is common in rocks.[14] The dimensionless ratio of these times characterizes the relaxation strength at the surface $\alpha = \tau_D/\tau_\rho = \rho a/D \sim 0.01$–$0.025$ (this is typically small). The gradient pulse is characterized by a "momentum" or inverse wavelength $\mathbf{k} = \gamma\delta\mathbf{g}$. The wavelength sets the scale of the structures probed. The inverse wave number $[1/(\gamma\delta g)]$ ranges from infinity (for $g=0$) to $23/2\pi$ μm for $\delta = 5$ ms, $g = 20$ G/cm.

Obviously, with the assumption of a single length scale, the time at which one starts seeing deviation from free diffusion (for zero or small momenta) is $\Delta \sim \tau_D$; this fact has been widely utilized or proposed to study the effects of restriction of diffusion.[7–11,19–23] To see the true asymptotic diffusion constant from the small-k data for a connected pore space, the walker would have to diffuse at least four or five typical pores (4×5 μm), for which it would take ~ 0.2 s, by which time the signal will have already decayed. Thus, in this case, it would be unrealistic to expect to obtain the true formation factor from the data.

If the pores were much smaller, however, the diffusion will have reached the asymptotic behavior, and there is some evidence for this, e.g., see Refs. 9 and 10. In these experiments however, $\sqrt{D\delta} \sim 1.4$ μm is larger than the pore size ~ 0.01 μm, i.e., the pulses are wider than the diffusion time τ_D. It is therefore clear that the expressions for the amplitude assuming δ-function pulses do not apply. What is worse is that it is not clear that the expressions for free diffusion, where correction has been made for finite pulse width, apply with the effective diffusion constant in place of the free diffusion constant. This, however, is the expression that has been used to analyze the experiments referred to.

As the relevant dimensionless momentum ka (or $k\sqrt{D\Delta}$ for a connected pore space) becomes large, one would expect to see deviation from quadratic behavior in k in the logarithm of the amplitude arising from the restricted diffusion, as seen in Ref. 23. The following interesting conclusion can be drawn from the dimensional analysis: if two samples were otherwise similar (geometry, etc.) and differed only by the basic length scale, then the amplitudes for experiments in the two rocks should collapse onto each other if plotted as a function of the dimensionless variables Δ/τ_D, $\gamma\delta ga$. For g small, this has been observed experimentally, e.g., see Ref. 19.

C. The cumulant expansion

The cumulant expansion provides a systematic way to gain information about the amplitude for small values of $k^2\langle r^2(\Delta)\rangle$. We have, in the random-walk language,

$$M(k,\Delta) = M(0,\Delta)\langle e^{i\mathbf{k}\cdot[\mathbf{r}(0)-\mathbf{r}(\Delta)]}\rangle, \tag{2.5}$$

where $M(0,\Delta)$ is the number of walkers surviving at time Δ, and has to be taken out so that the probability distribution given by the angle brackets is normalized (note that the subscript *un* has been dropped) to one at $k=0$ for all times. The odd terms vanish on averaging because the amplitude has to be real and the cumulant expansion gives

$$\ln\left(\frac{M(k,\Delta)}{M(0,\Delta)}\right)=\sum_{n=1}^{\infty}\frac{\langle\{i\mathbf{k}\cdot[\mathbf{r}(0)-\mathbf{r}(\Delta)]\}^{2n}\rangle_c}{(2n)!}, \tag{2.6}$$

where the cumulants are defined as usual, so that for $\langle X\rangle = 0$ one has

$$\langle X^2\rangle_c=\langle X^2\rangle,\quad \langle X^4\rangle_c=\langle X^4\rangle-3\langle X^2\rangle^2, \tag{2.7}$$

and so on.

The cumulant expansion formally truncates with the quadratic term in the case of free diffusion. This is because the measure in the sense of path integrals for free diffusion is a Gaussian, and higher-order cumulants vanish for a Gaussian distribution. In most existing studies, the influence of restricted geometry is taken into account[19–23,25–28] at the second-cumulant level (the assumption of a Gaussian distribution of phases is equivalent to this approximation). An important point of our paper is that it is possible to extract additional geometrical information from studying the k dependence beyond the lowest cumulant. The fact that the distribution of the total phase seen by a single random walker becomes non-Gaussian can already be seen from the effect of a single wall on the diffusion propagator: the propagator is the sum of two Gaussians for reflecting boundary conditions.[30]

D. The eigenfunction expansion

The Green's function defined in (2.2) is most conveniently written in terms of the eigenfunctions (for positive times)

$$G(\mathbf{r},\mathbf{r}',t)=\sum_{n=1}^{\infty}\psi_n(\mathbf{r})\psi_n(\mathbf{r}')e^{-t/T_n}, \tag{2.8}$$

where $\psi_n(\mathbf{r})$ are the normalized eigenfunctions of the equations

$$D\nabla^2\psi_n=-\frac{\psi_n}{T_n}, \tag{2.9}$$

$$D\hat{\mathbf{n}}\cdot\nabla\psi_n+\rho\psi_n\,|_{\mathbf{r}\in\Sigma}=0. \tag{2.10}$$

It follows from Eq. (2.1) that

$$M(k,\Delta)=\frac{1}{V}\sum_{n=1}^{\infty}|\tilde{\psi}_n(\mathbf{k})|^2e^{-\Delta/T_n}, \tag{2.11}$$

where

$$\tilde{\psi}_n(\mathbf{k})=\int d\mathbf{r}\,\psi_n(\mathbf{r})e^{-i\mathbf{k}\cdot\mathbf{r}}. \tag{2.12}$$

Note that, in absence of a field gradient, the decay is multiple exponential:

$$M(0,\Delta)=\frac{1}{V}\sum_{n=1}^{\infty}|\tilde{\psi}_n(0)|^2e^{-\Delta/T_n}, \tag{2.13}$$

$$\sum_{n=1}^{\infty}|\tilde{\psi}_n(0)|^2=V.$$

For $k=0$, Brownstein and Tarr[15] have given a similar eigenfunction expansion for simple isolated pores.

One can find a bound for the lowest eigenvalue using the standard variational approach [31] that a trial function (normalized) $\psi_{\rm tr}(\mathbf{r})$ gives

$$\frac{1}{T_0}\le D\int d\mathbf{r}|\nabla\psi_{\rm tr}(\mathbf{r})|^2+\rho\int dS|\psi_{\rm tr}(\mathbf{r})|^2. \tag{2.14}$$

The true minimum is the lowest eigenvalue, and the minimizing function is the corresponding eigenfunction. For $\rho\equiv 0$, the lowest eigenvalue is zero and the wave function is spatially constant. Taking this as the trial function $\psi_{\rm tr}=1/\sqrt{V}$ we find for the lowest mode

$$\frac{1}{T_0}\le\frac{\rho S}{V}. \tag{2.15}$$

For reflecting boundary conditions, and for a collection of isolated pores, the amplitude is trivially related to the "structure factors" of the isolated pores:

$$M(\mathbf{k},\infty)=\frac{1}{V^2}\sum_{\rm pores}\int d\mathbf{r}\,d\mathbf{r}'e^{-i\mathbf{k}\cdot(\mathbf{r}-\mathbf{r}')}. \tag{2.16}$$

III. THE k^2 DEPENDENCE OF AMPLITUDE AND DIFFUSION COEFFICIENT

In this section we use the cumulant expansion to study the k^2 dependent term which, for connected pore systems gives an effective diffusion coefficient. For isolated pores, the displacement is bounded above by the pore size, i.e., there is no diffusion. Consider the following cases (i) a single spherical pore of radius "a" and (ii) a connected pore space with a characteristic length "a."

From Eq. (2.6), the term quadratic in k is

$$\ln\left(\frac{M(k,\Delta)}{M(0,\Delta)}\right)=-\frac{\langle\{\mathbf{k}\cdot[\mathbf{r}(0)-\mathbf{r}(\Delta)]\}^2\rangle}{(2)!}. \tag{3.1}$$

If we assume the pore to be spherical, or if the angle brackets include an orientational average (as would be necessary in a model of an isotropic porous medium) we get in d dimensions

$$\ln\left(\frac{M(k,\Delta)}{M(0,\Delta)}\right)=-\frac{k^2\langle[\mathbf{r}(0)-\mathbf{r}(\Delta)]^2\rangle}{2d}. \tag{3.2}$$

For very short times $\Delta\ll\tau_D$, the typical walker has not "seen" the wall, and we have $\langle[\mathbf{r}(0)-\mathbf{r}(\Delta)]^2\rangle\approx 2dD\Delta$, leading to the usual result

$$\ln\left(\frac{M(k,\Delta)}{M(0,\Delta)}\right)=-k^2D\Delta. \tag{3.3}$$

In fact, this becomes exact as $\Delta\to 0$, since from Eqs. (2.1) and (2.2), it follows directly that

$$\lim_{\Delta\to 0}\frac{\partial\ln M(k,\Delta)}{\partial\Delta}=-Dk^2-\frac{\rho S}{V}. \tag{3.4}$$

Next consider the long time behavior. In case (i), only the lowest eigenfunction contributes to the normalized average represented by the angular brackets. One therefore has

$$\ln\left(\frac{M(k,\Delta)}{M(0,\Delta)}\right) = -C(\alpha)k^2a^2, \quad \alpha = \frac{\rho a}{D}, \tag{3.5}$$

where $C(\alpha)$ is a constant that depends on α, and is given by

$$C(\alpha) = \frac{1}{2d}\int [\mathbf{r}-\mathbf{r}']^2\psi(\mathbf{r})\psi(\mathbf{r}')d^dr\,d^dr', \tag{3.6}$$

where the integral is over the solid sphere of unit radius. In particular, we have

$$C(0) = \frac{1}{d+2}, \quad C(\infty) = \frac{1}{d}\left(1-\frac{2d}{\lambda_\infty^2}\right). \tag{3.7}$$

Here $C(0)$ has been calculated with the lowest eigenfunction for reflecting boundaries, which is constant. $C(\infty)$ has been computed using the lowest eigenfunction for absorbing boundary conditions, and the result is in terms of λ_∞ which is the lowest eigenvalue satisfying the equations

$$\frac{1}{r^{d-1}}\frac{d}{dr}r^{d-1}\frac{d}{dr}\psi(r) = -\lambda_\infty^2\psi(r), \quad \psi(r=1)=0,$$
$$\lambda_\infty = \frac{\pi}{2}, \quad 2.405, \quad \pi \quad \text{for } d = 1,2,3. \tag{3.8}$$

Note that $\alpha = 0$ and $\alpha = \infty$ corresponds to perfectly reflecting and perfectly absorbing boundary conditions, and intermediate values of α correspond to partially absorbing *bc*'s. The numerical constant changes by a factor of $C(0)/C(\infty)$ as one goes between the two extremes, and this ratio in $d = 1$, 2, 3, can be calculated from the above to be 1.76, 1.62, 1.53. The change, as one goes from perfectly reflecting to perfectly absorbing boundary conditions, is not even a factor of 2. Physically this is because the lowest normalized eigenfunction does not change very much in shape between the two extreme values: it goes from being flat for $\alpha = 0$ to hump shaped for $\alpha = \infty$.

We could put the above results together to give to leading order in the long time limit

$$M(k,\Delta) \propto \exp\left(-\lambda(\alpha)^2\frac{\Delta}{\tau_D}\right)\exp[-C(\alpha)k^2a^2],$$
$$\alpha = \frac{\rho a}{D}, \tag{3.9}$$

where C is a constant *weakly* dependent on ρ and $\lambda(\alpha)$ the lowest eigenvalue of the equation

$$\nabla^2\psi(\mathbf{r}) = -\lambda^2\psi(\mathbf{r}),$$
$$\hat{\mathbf{n}}\cdot\nabla\psi(\mathbf{r}) + \alpha\psi(\mathbf{r})|_{\mathbf{r}\epsilon\Sigma} = 0, \tag{3.10}$$

in notation defined earlier. Note that in this equation $\mathbf{r}$ is dimensionless. $\lambda(\alpha) \sim \sqrt{\alpha}$ for small α and $\lambda(\infty) = \lambda_\infty$ where λ_∞ is as defined above. The above conclusions obviously continue to hold for a convex-shaped pore space, as long as one carries out an orientational average (otherwise angular factors appear in the amplitude). The constraint on the shape could be relaxed to a certain extent without changing our conclusions.

Now consider the case of a connected pore space [case (ii)]. In the case $\rho = 0$, i.e., perfectly reflecting boundary conditions or zero wall relaxation, there is a one-to-one correspondence between the equations of motions *and* the boundary conditions of the present problem of diffusion of magnetization and the standard concentration diffusion in a porous medium. The effective diffusion coefficient in the latter problem is connected to the electrical conductivity via the standard Einstein relation.[29] If there is a well-defined macroscopic diffusion constant (which is not the case, for example, on a cluster at a percolation threshold), then one has rigorously

$$\lim_{\Delta\to\infty}\frac{[\mathbf{r}(0)-\mathbf{r}(\Delta)]^2}{2d\Delta} = D_{\text{eff}} = \frac{D}{F\phi}, \tag{3.11}$$

where F is the formation factor, which was defined in Eq. (1.3).

For finite ρ, guided by the results which we found for isolated pores, we can expect at times $\Delta \gg \tau_D$ and small k's that

$$M(k,\Delta) \propto \exp\left(-\lambda(\alpha)^2\frac{\Delta}{\tau_D}\right)\exp\left(-C_1(\alpha)k^2\frac{D}{F\phi}\Delta\right), \tag{3.12}$$

where $C_1(\alpha)$ is a numerical constant with $C_1(0) = 1$. We expect that for reasonably open geometries for the pore space, $C_1(\alpha)$ is only weakly dependent on α, and therefore it is reasonable to approximate it by 1 for weak surface relaxation. We could write our observation more precisely as

$$-\lim_{\Delta\to\infty}\frac{1}{\Delta}\frac{\partial\ln[M(k,\Delta)]}{\partial k^2}\bigg|_{k=0} = C_1(\alpha)\frac{D}{F\phi}, \tag{3.13}$$

where $C_1(\alpha) \approx 1$ for small values of α for reasonably open pore geometries. However, $C_1(\alpha)$ would be strongly dependent on α if, for example, there were long and narrow necks through which the walker has to pass in order to achieve its ultimate diffusive behavior. It is assumed that the number of walkers is normalized to one at each point of time. We are investigating the behavior of $C_1(\alpha)$ in some models of porous media, and the results will be reported elsewhere.

It has been already suggested in the literature that the pulsed gradient experiment could be used to determine the macroscopic diffusion constant and hence the formation factor (e.g., see Refs. 8–10). The above arguments provide theoretical justification why this should be the case. In particular the data of Fukuda *et al.*[9] can be explained using the above results and other known results on porous media. They find an "effective" diffusion constant which depends linearly on porosity. Assuming that Archie's "law"[32] holds in their case, i.e., $F = \phi^{-m}$, their data will be consistent with Archie's exponent $m = 2$, which is a reasonable value of m for their sintered glass bead samples.[33] However, as discussed above, theoretical expressions for the amplitude may fail to hold since the diffusion length during the application of the field gradient is comparable to the pore size.

We have discussed up to now only the lowest order term of the cumulant expansion. In the next two sections, we demonstrate that it is possible to extract additional geometrical information from studying k dependence beyond the lowest cumulant.

IV. THE k^4 TERM: ISOLATED PORES

In this section we show that the k dependence of the amplitude is a sensitive probe of the microgeometry. The quartic term is instructive, because it gives the first deviation from the quadratic behavior. For example, we show at long times the k^4 term could distinguish between (a) monodisperse spherical pores of radius a and (b) polydisperse spherical pores of radii distributed uniformly with mean $\langle a\rangle=0$ and range δa or (c) randomly oriented elliptic pores in $d=2$ with semimajor axes a and eccentricity ϵ (the effect of finite pulse widths may interfere with this application).

First consider a collection of spheres of the same size. We use the lowest eigenmode with the reflecting boundary condition to capture the essential physics at long times. Thus, the eigenfunction is constant throughout a pore and cumulants are easy to evaluate. It follows from a straightforward integration in d dimensions that

$$\langle[\mathbf{k}\cdot\mathbf{r}]^{2n}\rangle = k^{2n}a^{2n}\frac{\Gamma(\frac{d}{2}+1)(2n)!}{2^{2n}\Gamma(\frac{d}{2}+n+1)n!}. \tag{4.1}$$

Here the angular brackets mean an integration over the d-dimensional solid sphere, divided by its volume. The cumulant expansion, Eq. (2.6), using Eq. (4.1) gives

$$\lim_{\Delta\to\infty}\ln\left(\frac{M(k,\Delta)}{M(0,\Delta)}\right) = -\frac{k^2a^2}{d+2}-\frac{k^4a^4}{2(d+4)(d+2)^2} + O((ka)^6). \tag{4.2}$$

We could also write as

$$\lim_{\Delta\to\infty}\ln\left(\frac{M(k,\Delta)}{M(0,\Delta)}\right) = -C_1(d)k^2a^2 - C_2(d)k^4a^4, \tag{4.3}$$

with $C_1 = \frac{1}{3}, \frac{1}{4}, \frac{1}{5}$ and $C_2 = 1.1\times10^{-2}$, 5.2×10^{-3}, and 2.9×10^{-3} for $d=1$, 2, and 3, respectively. The higher-order terms are not illuminating.

Notice that the *sign* of the quartic term is negative, so that the amplitude decays faster than a quadratic in k. We show below that the sign can become different in cases (b) and (c). Thus, the sign of the initial curvature could be an experimental way of distinguishing between case (a) and the remaining cases. It is useful to bear in mind that the finite pulse widths could smear out the pore radius to some extent.

Let us now consider case (b), by doing a second average over the radius by means of an additional cumulant expansion. This gives

$$\lim_{\Delta\to\infty}\ln\left(\frac{M(k,\Delta)}{M(0,\Delta)}\right) = -C_1(d)k^2\langle a^2\rangle + \left(\frac{C_1^2(d)}{2}-C_2(d)\right)k^4\langle a^4\rangle - \frac{C_1^2(d)}{2}k^4\langle a^2\rangle^2 + O((ka)^6). \tag{4.4}$$

The quartic term changes sign when

$$\frac{\langle a^4\rangle-\langle a^2\rangle^2}{\langle a^2\rangle^2} = \frac{1}{d+3} = 0.42,\ 0.34,\ \text{and } 0.28 \text{ for } d=1,\ 2, \text{and } 3, \text{respectively}, \tag{4.5}$$

if we assume that the radii are uniformly distributed over the interval $a_0-\delta a/2, a_0+\delta a/2$ then the term changes sign when $\delta a/a_0$ is equal to 0.42, 0.34, 0.28 in $d=1$, 2, 3, e.g., in $d=3$ the logarithm of the amplitude plotted as a function of k^2 changes the curvature at the origin when the spheres become 28% polydisperse, and for more than 28% polydispersity, the logarithm of the amplitude decays *slower* than a quadratic in k.

Next consider case (c). The amplitude for a given orientation of the ellipse can be worked out as above up to the fourth cumulant, and then an orientational average can be done again in a cumulant expansion to yield

$$\lim_{\Delta\to\infty}\ln\left(\frac{M(k,\Delta)}{M(0,\Delta)}\right) = -\frac{k^2a^2}{4}\left(1-\frac{\epsilon^2}{2}\right) - \frac{k^4a^4}{192}\left(1-\epsilon^2-\frac{3\epsilon^4}{8}\right), \tag{4.6}$$

where a is the semimajor axis and ϵ the eccentricity. Again, it can be seen that the curvature at the origin changes sign when the ellipses have enough eccentricity, at $\epsilon=0.88$, which corresponds to a ratio of the semiminor to semimajor axis $b/a=0.47$. This result is due to a distribution of the lengths of the chords, in the direction of the gradient vector $\mathbf{g}$, drawn through the centers of the randomly oriented ellipses.

In cases (a), (b), and (c) we have used reflecting boundary conditions at the walls. However, the introduction of a partially absorbing boundary condition does not qualitatively alter our conclusions except for an overall normalization at zero k. Quantitatively, the results of Secs. III and VI show that the numerical constants used above are relatively insensitive to the values of ρ, and change, at most, by a factor of 2. In case (b) the same considerations should hold at finite ρ as long as the distribution of pore sizes is not too wide. The subtlety is that for a distribution of sphere sizes, different spheres will have different normalizations at zero k given by $\exp(-\rho\Delta/a)$, and then one might expect the conclusions above to change when the amplitude in the smallest pores is reduced by, say, a factor of 10 compared to the amplitude in the largest pores as a result of surface relaxation. This would happen when Δ has a value given by

$$\exp\left(\frac{\rho\Delta}{a_{\max}} - \frac{\rho\Delta}{a_{\min}}\right) \approx 0.1 \tag{4.7}$$

(assuming $\rho a/D$ small). However, at *fixed* Δ, if one was interested in the k dependence of the amplitude, then it is clear that the effect of a finite ρ is to put a cutoff on the distribution of radii. One would proceed exactly as before, only replacing the probability density function of radii $P(a)$ by $\exp(-\rho\Delta/a)P(a)$ for small values of $\rho a/D$. However, it needs to be emphasized that the existence of a broad distribution of length scales does not necessarily imply this cutoff on the distribution of sizes; this is only the case for *isolated* pores with a wide distribution of radii.

V. k DEPENDENCE ON MICROGEOMETRY IN CONNECTED PORES

In this section we describe a method of collapsing data for various k and Δ which reveals geometrical information, size, and connectivity, even when the decay of signal is strong enough such that the particles cannot diffuse distances long enough to give F. We show that this process can distinguish between a model of polydisperse spherical pores and randomly oriented tubes or sheets (to model the connected pore space). In the latter case the data would collapse as described below, while in the former case this would not happen. Also, the deviation from k^2 sets in at a much smaller value of k for the connected pore space than for isolated pores, because the important dimensionless number is $k^2D\Delta$ and not $(ka)^2$.

One of the principal motivations for this paper is to gain some understanding of the $\mathbf{k}$ dependence of the amplitude of a PFG experiment for fluids in a rock matrix. To do this we need a model of the pore space to which the walker is confined. In this context, the model that has been considered most widely is a collection of spherical pores with a distribution of radii.[6,23,28] This model captures the fact that the walkers are confined to a pore space. However, it misses an important part of the physics involved for a walker in the pore space of rocks: namely, at any point in the pore space, while there are directions in which the walker quickly hits the pore walls, there are also directions in which the walker can escape from the pore, and not be hindered at all. This consideration is important in this problem because what enters into the calculation of the amplitude is the restriction the walker sees *in the direction of field gradient* g. After long times, of course, the path of the walker becomes tortuous. However, if the observation times are not long enough for a single walker to sense the tortuosity of the pore space (which is quite likely to be the case, due to decay), then the only essential ingredient of a model of the pore space is that there be certain directions at a typical point in which the walker can diffuse freely for the observation time, while it hits the wall within the observation time in some other directions. To model the randomness of the pore space, these directions should be oriented randomly at different points.

Keeping these in mind, the simplest models one could think of are (a) a collection of randomly oriented tubes of the same radii and (b) a collection of randomly oriented sheetlike pores with the same thickness. Strictly speaking, the tubes do not intersect, but the results should not change much if they were allowed to intersect, provided the intersections do not form a significant fraction of the porosity, and the intersections are widely separated. There is a single parameter in the model, i.e., a length scale, namely, a tube radius or a sheet thickness.

Networks of tubes are quite commonly used to represent the pore structure of complex porous media (see numerous references cited, for example, in Dullien [29] and Mohanty[34]). In the context of a network of sheetlike pores we note that Wardlaw[35] has suggested that pores are often lamellar. Figure 2 shows a schematic representation of a rock with sheetlike pores. Incidentally, there exists a rich literature (see references in Cohen and Lin,[36] Mohanty[34]) on systematic methods to reduce a pore structure to its stripped down network starting from a micrograph. We would also like to note that the effect on the PFG amplitude of confining the walker to effectively lower dimensional spaces (sheets, tubes) oriented randomly has been considered in the past in a different context by Callaghan,[27] for confinement geometries that actually correspond to tubular or lamellar pore spaces.

First consider the model with cylinders of radii a, with axes oriented randomly. Equivalently, we consider a cylinder with the axis in the z direction with the gradient field being oriented randomly. For a fixed direction of the gradient field, we will make the second-cumulant approximation for the restricted diffusion along the radial directions, to obtain

$$\frac{M(k,\Delta)}{M(0,\Delta)} = e^{-k_z^2 D\Delta - (k_x^2+k_y^2)\langle r_\perp(\Delta)^2\rangle/4}, \tag{5.1}$$

where $r_\perp(\Delta)$ is the displacement of a walker perpendicular to the axis.

The displacement $r_\perp$ can be taken from Sec. III [or from the 2D equivalent of Eq. (6.6) below]. For small times, $\langle r_\perp(\Delta)^2\rangle/4 \sim D\Delta$, and for long times $\langle r_\perp(\Delta)^2\rangle/4 \sim a^2/4$ using the lowest eigenfunction for reflecting boundaries, which is a constant radially ($\Delta \leq$

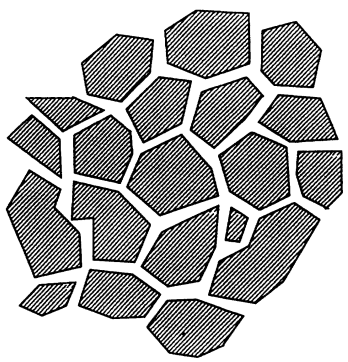

FIG. 2. An illustration of a rock with sheetlike pores.

a/ρ). Again, the essential physics is captured with this approximation, and the exact results given in the next section show that this approximation does not alter our conclusions. The crossover from the initial to the final form is exponential to the leading order, and to keep things simple, one can use the fitting form

$$\frac{\langle r_\perp(\Delta)^2\rangle}{4} = \frac{a^2}{4}\left[1-\exp\left(-\frac{4D\Delta}{a^2}\right)\right] \tag{5.2}$$

which has the right short- and long-time behaviors, and saturates exponentially.

Next, to see how good the second-cumulant approximation is for given ka, we could estimate the ratio of the fourth cumulant to the second. From Eq. (4.3), this is $0.012k^2a^2$, which for the parameter values considered in Sec. II ranges between 0 and 0.17, i.e., negligible.

Carrying out an average over orientations, Eq. (5.1) gives

$$\frac{M(k,\Delta)}{M(0,\Delta)} = e^{-D\Delta k^2}\int_0^1 e^{k^2[D\Delta-\langle r_\perp(\Delta)^2\rangle/4](1-x^2)}dx. \tag{5.3}$$

The amplitude is plotted in Fig. 3. It can be seen that the deviation from the k^2 behavior set in at a relatively small value of ka, as opposed to the isolated pores. The logarithm of Eq. (5.3) can be expanded to give

$$\ln\left(\frac{M(k,\Delta)}{M(0,\Delta)}\right) = -k^2\left(\frac{1}{3}D\Delta+\frac{2}{3}\frac{\langle r_\perp(\Delta)^2\rangle}{4}\right) + \frac{2}{45}k^4\left(D\Delta-\frac{\langle r_\perp(\Delta)^2\rangle}{4}\right)^2 + O((k^2D\Delta)^3). \tag{5.4}$$

It is clear by inspection that the model has the desirable short- and long-time behaviors, and embodies the appropriate tortuosity factor of $F\phi = 3$, corresponding to the effective diffusion being one dimensional.

Equation (5.3) has an important implication. Note that

$$\ln\left(\frac{M(k,\Delta)}{M(0,\Delta)}\right) + k^2D\Delta = f\left[k^2\left(D\Delta-\frac{\langle r_\perp(\Delta)^2\rangle}{4}\right)\right] \tag{5.5}$$

so that a somewhat model-independent prediction would be that different data sets of the logarithm of the normalized amplitudes with the amplitude for unrestricted diffusion subtracted out *should collapse* on a single curve when plotted against the variable $k^2[D\Delta-\langle r_\perp(\Delta)^2\rangle/4]$. A particularly simple fitting form for $\langle r_\perp(\Delta)^2\rangle$ is given by Eq. (5.2). There is a single unknown parameter a which could be adjusted to give the best fit, thus determining a length scale from the data. To reiterate, such collapse of data will not happen for isolated pores, even with a distribution of sizes.

The second model with randomly oriented sheetlike pores with thickness a is completely analogous to the above, and the above expressions are modified in this case to

$$\frac{M(k,\Delta)}{M(0,\Delta)} = e^{-D\Delta k^2}\int_0^1 e^{k^2[D\Delta-\langle r_\perp(\Delta)^2\rangle/2]x^2}dx \tag{5.6}$$

with

$$\frac{\langle r_\perp(\Delta)^2\rangle}{2} = \frac{a^2}{3}\left[1-\exp\left(-\frac{3D\Delta}{a^2}\right)\right]. \tag{5.7}$$

Plots of the amplitude are given in Fig. 4. The same remarks apply as in the case of tubes as regards extracting a length scale. Moreover, in these two cases the functional form of the amplitude is given, so that if the data collapsed as above, the functional form could be used to differentiate between the two microscopic geometries.

VI. EXACT RESULTS ON SIMPLE PORES

In this section we give the exact solutions for $M(k,\Delta)$ for arbitrary ρ for a slab and a sphere and a lamellar and a tubular pore. The main use of the exact results is to

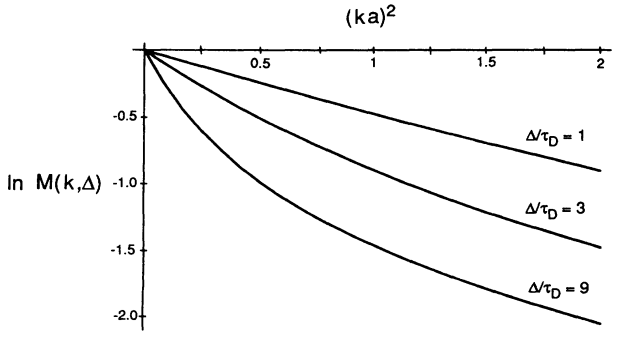

FIG. 3. The logarithm of magnetization normalized to its value for zero field gradient versus ka^2 for tubes of width a at various times $D\Delta/a^2 = 1, 3, 9$, respectively.

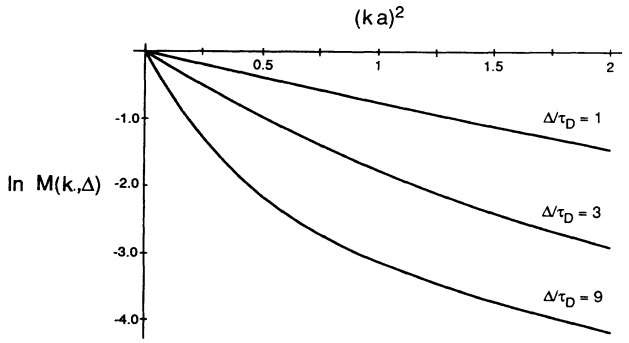

FIG. 4. The logarithm of magnetization normalized to its value for zero field gradient versus ka^2 for sheets of width a at various times $D\Delta/a^2 = 1, 3, 9$, respectively.

support our strategy of the previous sections where we used the lowest eigenmode with the reflecting boundary conditions to capture the essential physics.

A. Slab-shaped pore

First consider a one-dimensional case. We take a region bounded between $z = 0, 2a$, with surface relaxation only at $z = 2a$, so that the eigenfunctions and eigenvalues are

$$\psi_n = N_n \cos(\xi_n z/2a), \quad \frac{1}{T_n} = \frac{D\xi_n^2}{4a^2}, \tag{6.1}$$

where N_n is the normaliztion constant and ξ_n are positive roots of the

$$\xi_n \tan\xi_n = 2\rho a/D. \tag{6.2}$$

We find by a straightforward integration from Eqs. (2.17) and (6.1) that

$$|\tilde{\psi}_n(k)|^2 = \frac{4\xi_n}{2\xi_n + \sin(2\xi_n)} \frac{1}{(\xi_n^2 - 4k^2a^2)^2} \{4k^2a^2[1 + \cos^2\xi_n - 2\cos\xi_n \cos(2ka)] - 4ka\xi_n \sin\xi_n \sin(2ka) + \xi_n^2 \sin^2\xi_n\}. \tag{6.3}$$

The amplitude $M(k, \Delta)$ follows from Eqs. (2.11) and (6.3) For $g = 0$, i.e., no field gradient, we recover the results of Brownstein and Tarr,[15] namely,

$$|\tilde{\psi}_n(0)|^2 = \frac{4\sin^2\xi_n}{\xi_n[2\xi_n + \sin(2\xi_n)]}. \tag{6.4}$$

In the case of $\rho = 0$ (reflecting boundary conditions) we have $\xi_n = n\pi$, $n = 0, 1, 2, \ldots$, which gives for the amplitude

$$M(k, \Delta) = \frac{\sin^2(ka)}{(ka)^2} + \sum_{n=1}^{\infty} \frac{16e^{-D\Delta n^2\pi^2/4a^2} k^2a^2}{(n^2\pi^2 - 4k^2a^2)^2}[1 - (-1)^n \cos(2ka)] \tag{6.5}$$

which is identical to Eq. (88) of Ref. 2. For $\rho = \infty$ (absorbing boundary conditions), the positive roots are given by $\xi_n = (n + 1/2)\pi, n = 0, 1, \ldots$. The expression is different from Eq. (10) in Ref. 3, because here one surface was assumed active.

The mean-squared displacement is

$$\langle |z(\Delta) - z(0)|^2 \rangle = \frac{8a^2}{\sum_{n=0}^{\infty} |\tilde{\psi}_n(0)|^2 e^{-t/T_n}} \sum_{n=0}^{\infty} 4e^{-t/T_n} \frac{\xi_n \sin\xi_n - \sin^2\xi_n + 2\cos\xi_n - 2}{\xi_n^3[2\xi_n + \sin(2\xi_n)]}. \tag{6.6}$$

Note that the quantity

$$\frac{\langle |z(\Delta) - z(0)|^2 \rangle}{2D\Delta}$$

has the right long- and short-time behaviors, as in Eq. (5.7).

For long times and small values of ka, the results consistent with the cumulant expansion are recovered as expected. One could consider the limiting cases of weak and strong surface relaxivity: (i) weak relaxivity ("fast diffusion limit"[15] for the relaxation enhancement) $\rho a/D \ll 1 : T_0 \approx 2a/\rho$, and for long times

$$M(k, \Delta) \approx e^{-\frac{\rho}{2a}\Delta} e^{-k^2a^2/3}. \tag{6.7}$$

(ii) Strong relaxivity ("slow diffusion limit"), $\rho a/D \gg 1$, and for long times

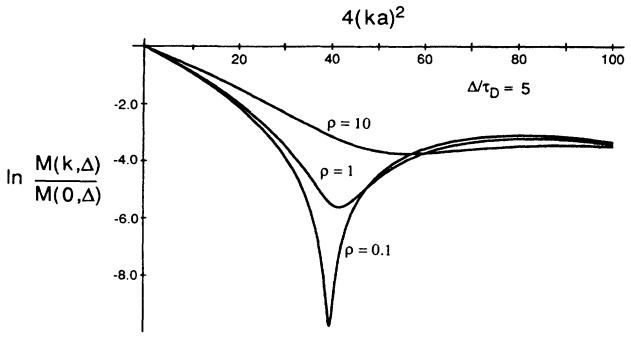

FIG. 5. Exact solution for parallel plates for $\rho = 0.1, 1, 10$ versus $4k^2a^2$ for width $2a$ at time $D\Delta/4a^2 = 5$.

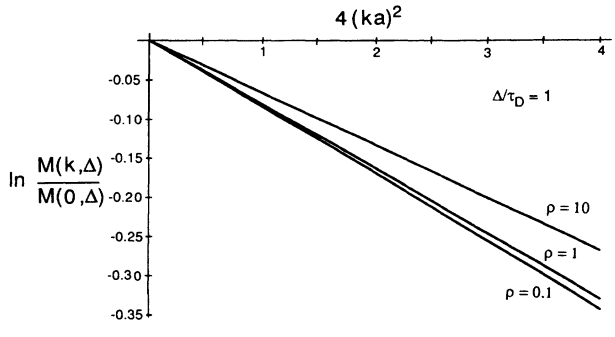

FIG. 6. Same as Fig. 4, at $D\Delta/4a^2 = 1$, the range of k has been reduced.

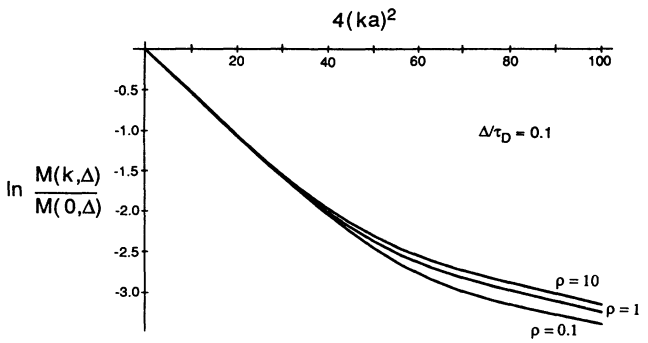

FIG. 7. Same as Fig. 4, at $D\Delta/4a^2 = 0.1$.

$$M(k,\Delta) \approx \frac{8}{\pi^2} e^{-(D\pi^2/16a^2)\Delta} e^{-16k^2a^2(\pi-3)/\pi^2}. \quad (6.8)$$

The numerical constant multiplying $(ka)^2$ is different from the result of the cumulant expansion because only one surface is active.

The exact solutions support our claim that the normalized amplitude depends weakly on ρ, cf. Figs. 6 and 7. In Fig. 5, there is an oscillation in the amplitude which dies away as ρ increases. This oscillation is due to a resonance when a wavelength fits in the slab. The effect will be reduced when there is a random orientation or a polydipersity in pore sizes. It is also possible that the finiteness of the pulse widths will also smear out the oscillation. When these difficulties are not present, these oscillations can be useful probes for monodisperse clean pores. The statement about the ρ dependence of the amplitude should be qualified in the presence of these oscillations; the precise statement is that the normalized amplitude depends weakly on ρ *except* when a resonance condition is satisfied $ka \sim n, d = 1$.

B. Spherical pore

In this case there is rotational symmetry about the direction of the field gradient and the eigenfunctions are

$$\psi_{l,n} = N_{ln} j_l(\zeta_{ln} r/a) Y_{l0}(\theta,\phi), \quad \frac{1}{T_{ln}} = \frac{D\zeta_{ln}^2}{a^2}. \quad (6.9)$$

Here we choose the convention and normalizations as given in Jackson's[37] book on electrodynamics, so that j_l are spherical Bessel function of order l and Y_{lm} are spherical harmonics. The normalization constant is N_n and the root ζ_{ln} corresponds to the nth root of the equation

$$\zeta_{ln} j_l'(\zeta_{ln}) = -\frac{\rho a}{D} j_l(\zeta_{ln}). \quad (6.10)$$

Using the standard expansion of e^{-ikz} as given by Eq. (16.129) of Jackson's book,[37] we find, after a straightforward integration that

$$M(k,\Delta) = \sum_{ln=0}^{\infty} \frac{6(2l+1)\zeta_{ln}^2 e^{-D\Delta\zeta_{ln}^2/a^2}}{(\zeta_{ln}^2 - k^2a^2)^2} \times \frac{kaj_l'(ka) + \frac{\rho a}{D} j_l(ka)}{\left(\frac{\rho a}{D} - \frac{1}{2}\right)^2 + \zeta_{ln}^2 - (l+1/2)^2}. \quad (6.11)$$

For the limiting cases as above, for long times and small ka the above expression gives

$$M(k,\Delta) \approx e^{-(3\rho/D)\Delta} e^{-k^2a^2/5} \quad (6.12)$$

in the fast diffusion limit, and

$$M(k,\Delta) \approx \frac{6}{\pi^2} e^{-(D\pi^2/4a^2)\Delta} e^{-k^2a^2(\pi^2-6)/3\pi^2} \quad (6.13)$$

in the slow diffusion limit.

C. Lamellar pore

For simple shapes, such as lamella or tubes, the separation of variables is elementary and the exact result for the lamallar pore can be written down by inspection (for a sheet in the x-y plane and an arbitrary $\mathbf{k}$)

$$\frac{M(k,\Delta)}{M(0,\Delta)} = e^{-k_\perp^2 D\Delta} \frac{\sum_{n=1}^{\infty} |\tilde{\psi}_n(k_z)|^2 e^{-\Delta/T_n}}{\sum_{n=0}^{\infty} |\tilde{\psi}_n(0)|^2 e^{-\Delta/T_n}}. \quad (6.14)$$

Here ψ_n are the eigenfunctions and T_n are the eigenvalues in the one-dimensional problem, which was discussed above.

D. Mean lifetime

It has been shown recently[38] that the problem of magnetization decay in the presence of surface relaxers (equivalent to the normalization at zero k in our problem) simplifies greatly if one is interested only in the mean lifetime τ_m [note that $M(t=0) = 1$ is the normalization used]

$$\tau_m = \int_0^{\infty} M(t)dt. \quad (6.15)$$

For spherical pores in $d = 1, 3$ the mean lifetimes are[38]

$$\tau_m(\rho, D) = C_1\tau_D + C_2\tau_\rho \quad (6.16)$$

with $C_1 = \frac{1}{3}, \frac{1}{15}$, and $C_2 = 1, \frac{1}{3}$ in $d = 1, 2$. This unexpected simplification arises from symmetry and the initial condition of homogeneous magnetization. In our problem, for the mean lifetime, similar simplification occurs only in $d = 1$, and the expression for the mean lifetime for the sphere is only obtainable as a series expansion. The mean lifetime in case of finite k can be calculated as follows:

$$\tau_m(k) = \int_0^{\infty} M(\mathbf{k},\Delta)d\Delta \quad (6.17)$$

equals the $s = 0$ value of the Laplace transform

$$\widetilde{M}(\mathbf{k},s) = \int_0^{\infty} M(\mathbf{k},t)e^{-st}dt. \quad (6.18)$$

The Laplace transform of the magnetization with $s = 0$ satisfies

$$D\nabla^2 \widetilde{M}(\mathbf{r}, s = 0) = -e^{-i\mathbf{k}\cdot\mathbf{r}} \tag{6.19}$$

with the boundary condition at the pore wall:

$$D\hat{\mathbf{n}} \cdot \boldsymbol{\nabla} \widetilde{M} + \rho \widetilde{M} \mid_{\mathbf{r}\epsilon\Sigma} = 0, \tag{6.20}$$

where we have neglected diffusion during the duration δ of the first pulse. Thus,

$$\tau_m(k) = \int d\mathbf{r}\, e^{i\mathbf{k}\cdot\mathbf{r}} \widetilde{M}(\mathbf{r}, s = 0). \tag{6.21}$$

For a planar pore with $\mathbf{k}$ normal to the planes bounding the pore we obtain

$$\tau_m(k) = \frac{2}{(ka)^2}\left[\frac{a^2}{D}\left(1 - \frac{\sin(ka)}{ka}\right) + \frac{a}{\rho}[1 - \cos(ka)]\right]. \tag{6.22}$$

The lifetime separates in a ρ dependent part and a D dependent part. In principle, with the aid of the above expression, it is possible to determine ρ and a separately, given D. For example, for small $ka << 1$, we find

$$\tau_m(k) = \left(\frac{a^2}{3D} + \frac{a}{\rho}\right) - \frac{k^2a^2}{12}\left(\frac{a^2}{5D} + \frac{a}{\rho}\right). \tag{6.23}$$

For the spherical pore we obtain

$$\tau_m(k) = \frac{1}{Dk^2}\left[1 - 3\sum_l \frac{2l+1}{ka}\left(j_{l+1}(ka)j_l(ka) - \frac{kaj_{l+1}^2(ka)}{l + \rho a/D}\right)\right]. \tag{6.24}$$

Only for $l = 0$ do the ρ- and D-dependent terms separate, because the field gradient breaks the spherical symmetry.

Using the Cauchy-Schwartz inequality, one can prove an inequality in the usual way relating the initial decay rate $1/\tau_{in}(k) = Dk^2 + \rho S/V$ and the mean lifetime $\tau_m(k)$:

$$\frac{1}{\tau_{in}(k)}\tau_m(k) \geq 1 \quad \text{or} \quad \tau_m(k) \geq \frac{1}{Dk^2 + \frac{\rho S}{V}}.$$

VII. EFFECTS OF RANDOM LOCAL FIELDS

The main purpose of this paper was to show how the k dependence of the stimulated echo amplitude contains information about the microgeometry. To keep matters simple we made the important assumption that $\delta, \tau_1 \to 0$, and this allowed us to assume that there was no significant phase evolution in the random local field during τ_1 (see Fig. 1). We now discuss this point further.

When a porous medium, such as sandstone, is placed in a homogeneous magnetic field, the internal local magnetic field is generally inhomogeneous, i.e., varies from point to point. This arises due to a difference between the magnetic susceptibility of the grain and the pore fluid.

A simple expression for the pulsed echo amplitude in presence of internal magnetic field inhomogeneities can be given if one makes the assumption that these inhomogeneities are weak compared to the uniform static field. This is a good approximation because the internal field inhomogeneities are created by the susceptibility difference which is typically of the order of 10^{-5} in the materials dicussed here.[12] In this limit, when one transforms to the rotating frame, only the components of the internal field inhomogeneities parallel to the static external field survive. The components transverse to the external field rotate very fast and may be neglected. Thus, we need only consider the local inhomogeneities in Larmor frequency. Let the local Larmor frequency be $\omega_0 + \omega(\mathbf{r})$ where $\omega(\mathbf{r})/\omega_0$ is small. For the pulse sequence as illustrated in Fig. 1, the amplitude $M_{in}(k, \Delta)$ is

$$M_{in}(k, \Delta) = \int d\mathbf{r}\, d\mathbf{r}' e^{i\mathbf{k}\cdot(\mathbf{r}-\mathbf{r}')} G(\mathbf{r}, \mathbf{r}'; \Delta) e^{i\tau_1[\omega(\mathbf{r})-\omega(\mathbf{r}')]}.$$

The above expression follows if one assumes that δ, τ_1 are so short that the spins do not significantly diffuse during those intervals. For the illustrated pulse sequence, an overall factor of $\exp[-2\tau_1/T_{2B} - (\tau_2 - \tau_1)/T_{1B}]$ is implied. This equation differs from Eq. (2.1) in that the spin picks up a phase $\tau_1\omega(\mathbf{r})$ between the first two $\pi/2$ pulses and a phase $\tau_1\omega(\mathbf{r}')$ after the third $\pi/2$ pulse from the internal inhomogeneous Larmor frequency. They come with opposing signs because the two $\pi/2$ pulses effectively reverse the sign of the first phase. In the literature, one usually finds the case of a constant background gradient $\mathbf{g_0}$, i.e., $\omega(\mathbf{r}) = \gamma \mathbf{g_0} \cdot \mathbf{r}$.

The above more general expression is not amenable to exact analysis in an arbitrary porous medium. However, it is clear from the expression that when random local fields are present, the k dependence of $M(k, \Delta)$ is different from that of the Fourier transform of the propagator discussed in the paper. This is true even in the case of free diffusion in the presence of a constant background gradient, as can be seen from the exact solutions in this case given by Tanner.[22] We are currently analyzing the above expression to investigate quantitatively how the k dependence changes. The random local fields can produce nontrivial effects in the time dependence of a Hahn echo.[39]

VIII. CONCLUSIONS AND DISCUSSIONS

We have proposed that the "momentum" $(\gamma\delta g)$ dependence of the amplitude in a pulsed-field-gradient experiment for fluids in a porous medium at fixed time is a sensitive structural probe of the microgeometry of the porous medium, for features in the range of length scales lying between the diffusion length $l_D = \sqrt{D\Delta}$ and the characteristic length associated with a gradient pulse $1/(\gamma\delta g)$. We have shown that the k dependence could be used to distinguish between monodisperse spherical pores and sufficiently polydisperse spherical pores or randomly oriented anisotropic shaped pores. We have shown that the k dependence can distinguish between isolated pores

and pore geometries where there locally exist directions in which the walker can diffuse freely during the observation time. This is achieved by means of a certain data collapse as described in the text. We have used simple models consisting of collections of randomly oriented tubes or sheets to interpret the k dependence of the amplitude in rocks. We have given the exact solutions for the amplitude for a planar pore and for a sphere with partially absorbing boundary conditions corresponding to surface relaxation, and have concluded that for isolated convex-shaped pores with a single characteristic size, the amplitude is only weakly dependent on the strength of the surface relaxation apart from an overall normalization that decays in time. For a connected pore space, we have discussed cases where we also expect similar results to hold.

The following experiments could test whether the normalized amplitude $M(k,\Delta)/M(0,\Delta)$ as a function of k has a weak ρ dependence for a given sample. Let us assume that the sample is water wet (hydrophillic). First saturate it with hydrocarbon while leaving a thin layer of water behind, such that the hydrocarbon does not come into direct contact with the paramagnetic impurities on the pore wall. In this case the hydrocarbon protons will not suffer enhanced relaxation, i.e., $\rho \approx 0$. Next repeat the experiment, except, first remove all water by drying the sample thoroughly. Now the influence of the surface will be non-negligible, and $M(0,\Delta)$ should change. But if the pores are not connected by long thin necks, we expect $M(k,\Delta)/M(0,\Delta)$ will be about the same in both cases. A similar experiment can be done by measuring $M(k,\Delta)/M(0,\Delta)$ on deuterium in a fully D_2O-saturated rock and by comparing it with $M(k,\Delta)/M(0,\Delta)$ of proton when the same rock is fully saturated with water. Influence of paramagnetic impurities is much smaller on deuterium than on proton. As discussed above, a strong ρ dependence will have some implications on the sample geometry.

Deviation of $\ln M(k,\Delta)$ from k^2 behavior can result from various reasons and has been seen in experiments. In some systems,[2,3,40] the fluid diffuses with different diffusion coefficients in different compartments. In those cases, $M(k,\Delta)$ is a sum of Gaussians, which can give rise to a significant deviation from k^2 behavior, but this is not the kind of effect we are considering in the present paper. As we have mentioned already, Callaghan and his coworkers,[27,28] studied systems where the fluid is confined between lamella of aerosol or in biological tissues (wheat endosperm) with tube-shaped pores. There the deviation of quadratic behavior arises from locally anisotropic diffusion. The diffusion is hindered in one (two) direction(s) and free in the other direction(s). The directions of free diffusion are randomly oriented in different parts of the sample. In porous media, we have argued that a similar combination of hindered and free diffusion will give rise to the deviation of $M(k,\Delta)$ from k^2 behavior. It can be seen that the data of Lipsicas,[6] has a rather nonlinear dependence on k^2. The data at different times, Δ should collapse onto a form similar to Eq. (5.5), but the data was not available to test this idea.

There are several examples in the literature, where the NMR has been used to study the morphology of microemulsions, especially the transition where one of the components undergoes a change between being disconnected to being continuous. Callaghan *et al.*[41] have used the diffusion coefficient to delineate such phase boundaries, but as we have argued above, the full k dependence will be even more informative.

The subject of study in this paper, i.e., the momentum dependence of the diffusion propagator in a porous medium, can be observed experimentally by dynamical light scattering experiments.[42] In these experiments, a significant curvature is seen for $\ln[G(k,t)]$ as a function of k^2 in the appropriate parameter ranges.

After we submitted this paper, it was brought to our notice that the presence of microscopic structural information in the pulsed-field-gradient amplitude has been vividly demonstrated in experiments by Cory and Garroway[43] in isolated pores, and by Callaghan *et al.*[44] in packings of polystyrene spheres. It has been emphasized[45] that in these experiments the gradient pulse plays the role of a wave vector probing the structure of the obstacles to the diffusion. The spatial Fourier transform of the experimental profiles provide dramatic illustration of the structural information present in the signal. Callaghan *et al.*[44] present a model of weakly coupled identical pores to interpret their data. Our analysis for a connected geometry led us to a somewhat different phenomenological expression, which will be considered elsewhere.

ACKNOWLEDGMENTS

We are grateful to R. Kleinberg and L. Latour for providing us with some data, prior to publication, which was crucial in motivating this work. We thank them and B. I. Halperin, P. Le Doussal, L. Schwartz, D. L. Johnson, R. A. Guyer, T. S. Ramakrishnan, D. Wilkinson, A. Sezginer, and M. Lipsicas for useful discussions.

*Permanent address: Department of Physics, Harvard University, Cambridge, MA 02138.

[1] E. L. Hahn, Phys. Rev. **80**, 580 (1950); H. Y. Carr and E. M. Purcell, *ibid.* **94**, 630 (1954); T. P. Das and A. K. Saha, *ibid.* **93**, 749 (1954).

[2] J. Karger, H. Pfeifer and W. Heink, in *Advances in Magnetic Resonance*, edited by J. S. Waugh (Academic, San Diego, 1981), Vol. 12, p. 1.

[3] S. Frey, J. Karger, H. Pfeifer, and P. Walther, J. Magn. Reson. **79**, 336 (1988).

[4] D. E. Woessner, J. Phys. Chem. **67**, 1365 (1963).

[5] K. J. Packar, C. Rees, and D. J. Tomlinson, Adv. Mol. Relaxation Process **3**, 119 (1972).

[6] M. Lipsicas, J. R. Banavar, and J. Willemesen, Appl. Phys. Lett. **48**, 1544 (1986).

[7] P. G. de Gennes, C. R. Acad. Sci. **295**, 1061 (1982).

[8] H. J. Vinegar and W. P. Rothwell, U.S. Patent No. 4719423 (1988), filed (1985).

[9] K. Fukuda, T. T. Kasuga, T. Mizusaki, A. Hirai, and K. Eguchi, J. Phys. Soc. Jpn. **58**, 1662 (1989), and references therein.
[10] F. D'Orazio, S. Bhattacharja, W. P. Halperin, and R. Gerhardt, Phys. Rev. **42**, 6503 (1990), and references therein.
[11] See, for example, papers in *Transport and Relaxation in Random Materials*, edited by J. Klafter, R. J. Rubin, and M. F. Shlesinger (World Scientific, Singapore, 1986).
[12] R. L. Kleinberg and M. A. Horsfield, J. Magn. Reson. **88**, 9 (1990), and references therein.
[13] M. H. Cohen and K. S. Mendelson, J. Appl. Phys. **53**, 1127 (1982); K. S. Mendelson, Phys. Rev. B **41**, 562 (1990).
[14] W. Kenyon, J. Howard, A. Sezginer, C. Straley, A. Matteson, K. Horkowitz, and R. E. Ehrlich (unpublished).
[15] K. R. Brownstein and C. E. Tarr, Phys. Rev. A **19**, 2446 (1979).
[16] D. O. Seevers (unpublished).
[17] C. H. Neuman and R. J. S. Brown, J. Pet. Technol. **xx**, 2853 (1982); A. Timur, *ibid.* **21**, 775 (1969).
[18] R. J. S. Brown, Nature (London) **189**, 388 (1961).
[19] R. C. Wayne and R. M. Cotts, Phys. Rev. **151**, 264 (1966).
[20] B. Robertson, Phys. Rev. **151**, 273 (1966); **3**, 119 (1972).
[21] E. O. Stejskal and J. E. Tanner, J. Chem. Phys. **42**, 288 (1965); E. O. Stejskal, *ibid.* **43**, 3597 (1965).
[22] J. E. Tanner, J. Chem. Phys. **52**, 2523 (1970).
[23] J. E. Tanner and E. O. Stejskal, J. Chem. Phys. **49**, 1768 (1968).
[24] R. F. Karlicek, Jr. and I. J. Lowe, J. Magn. Reson. **37**, 75 (1980); R. M. Cotts, M. J. R. Hoch, T. Sun, and J. T. Marker, *ibid.* **83**, 252 (1989).
[25] C. H. Neumann, J. Chem. Phys. **60**, 4508 (1974).
[26] J. S. Murday and R. M. Cotts, J. Chem. Phys. **48**, 4938 (1968).
[27] P. T. Callaghan and O. Soderman, J. Phys. Chem. **87**, 1737 (1983).
[28] P. T. Callaghan, K. W. Jolly, and R. S. Humphrey, J. Colloid Interface Sci. **93**, 521 (1982).
[29] F. A. L. Dullien, *Porous Media* (Academic, New York, 1979).
[30] S. Chandrasekhar, Rev. Mod. Phys. **15**, 1 (1943).
[31] J. W. Dettman, *Mathematical Methods in Physics and Engineering* (McGraw-Hill, New York, 1962).
[32] G. E. Archie, Trans. AIME **146**, 54 (1942).
[33] J. N. Roberts and L. Schwartz, Phys. Rev. B **31**, 5990 (1985).
[34] K. K. Mohanty, Ph.D. thesis, University of Minnesota, 1981 (unpublished).
[35] N. C. Wardlaw and J. P. Cassan, Bull. Canad. Petrol. Geo. **26**, 572 (1978).
[36] M. H. Cohen and C. Lin, in *Macroscopic Properties of Porous Media*, Springer Lecture Notes in Physics, No. 154 1982, G. Papanicolau and R. Burridge (Springer-Verlag, New York, 1982).
[37] J. D. Jackson, *Classical Electrodynamics*, 2nd ed. (Wiley, New York, 1977).
[38] D. Wilkinson, D. L. Johnson, and L. M. Schwartz, Phys. Rev. B **44**, 4960 (1991).
[39] P. M. Mitra, P. Le Doussal, and B. I. Halperin (unpublished).
[40] E. Von Meerwall, D. Mahoney, G. Innacchione, and D. Skowronski, J. Colloid Interface Sci. **139**, 437 (1990).
[41] P. T. Callaghan, K. W. Jolly, and J. Lelievre, Biophys. J. **28**, 133 (1979).
[42] M. T. Bishop, Ph.D. thesis, University of Massachusetts, 1987 (unpublished).
[43] D. Corey and A. Garroway, Magn. Reson. Medicine **14**, 435 (1990).
[44] P. T. Callaghan, D. MacGowan, K. J. Packer, and F. O. Zelaya, Nature (London) **351**, 443 (1991); J. Magn. Reson. **90**, 177 (1990).
[45] R. M. Cotts, Nature (London) **351**, 443 (1991).